BEHAVIOUR OF A ONE TON ROTOR BEING DROPPED INTO AUXILIARY BEARINGS

J. SCHMIED AND J. C. PRADETTO
Sulzer Escher Wyss Ltd.
Escher Wyss Platz
CH 8023 Zürich, Switzerland

REPRINTED FROM **PROCEEDINGS OF THE THIRD INTERNATIONAL SYMPOSIUM ON MAGNETIC BEARINGS**
JULY 29 31, 1992

Behaviour of a One Ton Rotor Being Dropped into Auxiliary Bearings

J. SCHMIED AND J. C. PRADETTO
Sulzer Escher Wyss Ltd.
Escher Wyss Platz
CH 8023 Zürich, Switzerland

ABSTRACT

The vibrational behaviour of a one ton compressor rotor being dropped into the auxiliary bearings in case of a failure of its magnetic bearings is reported. The auxiliary bearings are ball bearings with a clearance between rotor and inner race. The results are based on tests and theoretical investigations. The most critical condition, which can occur, is a whirling motion of the rotor with approximately the clearance as the radius of the orbit. A whirling for an extended period of time must be prevented by an appropriate design.

INTRODUCTION

At the last Magnetic Bearing Conference in Tokyo we reported about a hermetically sealed motor pipeline compressor (MOPICO) [1] representing todays extreme combination of speed and weight concerning magnetic bearing applications (fig.1). The fully integrated design of this

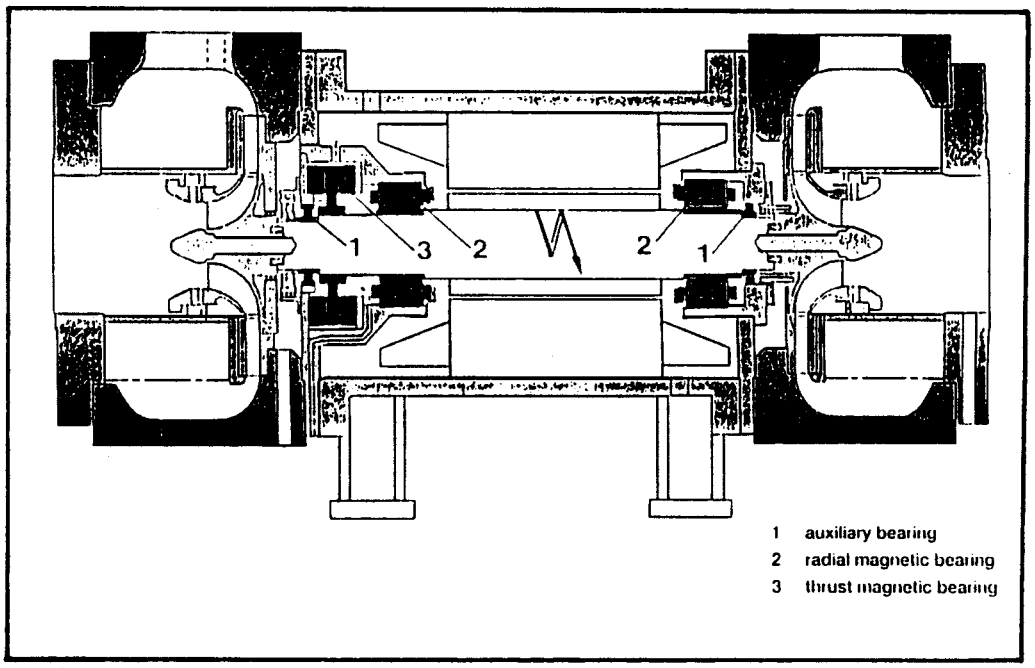

Figure 1. Cross section of the MOPICO

compressor could be realized thanks to the development of a high speed motor, which is in the middle of the rotor, and thanks to magnetic bearings. Both bearings and motor are totally submerged in the natural gas working fluid.

In the Tokyo paper we concentrated on the rotordynamic behaviour of the machine regularly running in magnetic bearings. The modeling of the magnetic bearings, theoretical results, such as natural frequencies, damping factors and transfer functions, as well as test results gained during the development were described.

In the present paper the rotordynamic behaviour in case of a magnetic bearing failure is presented. In this case the rotor is dropped into the auxiliary bearings, which are ball bearings with a clearance between rotor and inner race. The vibrational behaviour of this event was investigated theoretically and experimentally on the real machine at almost full speed and load. Results of both investigations are reported. In the theoretical investigations the influence of some parameters on the behaviour were studied and some general rules could be deduced.

MODELING THE ROTOR AUXILIARY BEARING SYSTEM

THE ROTOR

The basic data of the rotor are as follows:

Weight:	1 ton
Length:	app. 2 m
Maximum speed:	10000 rpm
Frequency of the first bending mode at standstill (unsupported):	11000 rpm

For the theoretical investigations the rotor was modeled by finite elements. The model consists of 21 elastic shaft elements and three rigid disks.

THE AUXILIARY BEARINGS

At standstill and in the case of a power failure of the magnetic bearings the rotor is supported on the auxiliary ball bearings (fig.2). One of them is a combined radial and thrust bearing. The gap between the inner race of the bearing and the rotor is approximately half the gap between the

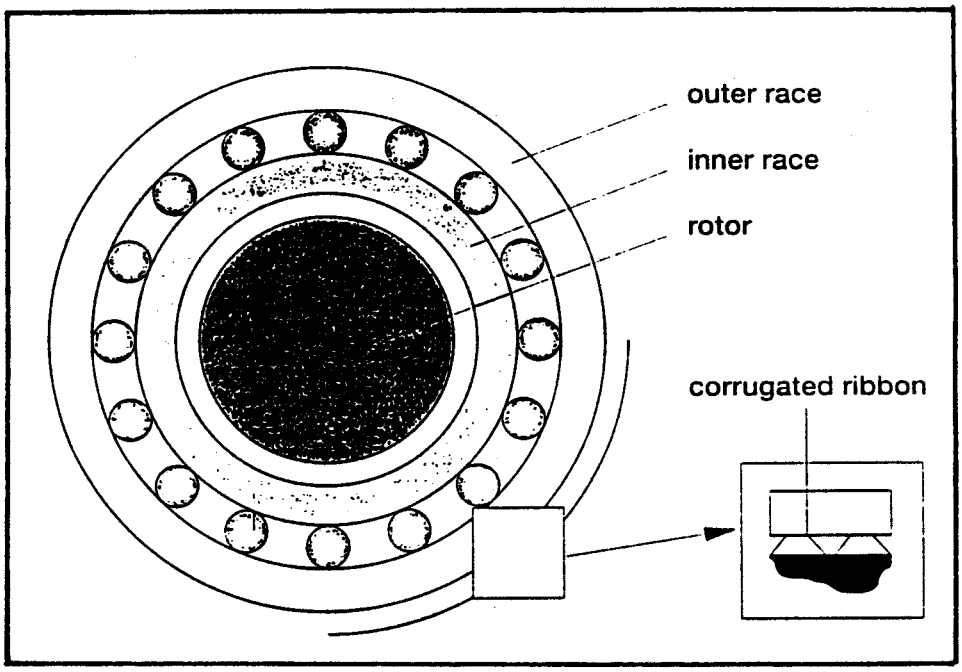

Figure 2.
Scheme of the auxiliary bearings

rotor and the stator of the magnetic bearing. A corrugated ribbon is inserted between the outer race and the housing for damping reasons.

In the power failure case the drive is shut down immediately and the rotor is decelerated very fast by the aerodynamic forces on the impellers. The deceleration of the speed due to the aerodynamic torque can be described by the following function:

$$n = n_0 / (1 + at) \tag{1}$$

n_0 speed at the instant of the failure
t time from the instant of the failure
a deceleration factor, which depends on the load (at full load a = 0.5 1/s)

For the rotor drop case the force from the auxiliary bearing on the rotor is modeled by nonlinear forces, which take into account the elasticity and damping of the ball bearing and the corrugated ribbon as well as the friction between the rotor and the inner race. The following assumptions are made for the description of the forces:

a) The lateral inertia forces of the auxiliary bearing are negligible. Only the polar moment of inertia of the inner race including balls and cage is taken into account.
b) The ball bearing and corrugated ribbon have a stiffness and damping force in radial direction. Additionally, the corrugated ribbon has a damping force in circumferential direction. The housing is assumed as rigid.
c) The rolling friction coefficient is negligible.
d) The relative velocity at the contact point between inner ring and rotor is only determined by the circumferential velocities due to the rotational speeds. The influence of the lateral rotor and ring motion is neglected, since the deflections of both are much smaller than the radius of the shaft and the inner race.
e) The friction force between rotor and inner race acts only on the rotor as long as the rotational speed of the inner race is smaller than the rotor speed. Once the rotational speed of the inner ring (which is normally zero at the instant of a failure) is accelerated by the rotor up to the same speed, there is no relative velocity between both, hence there is no more friction.
f) The friction force between rotor and inner race does not influence the decelerating rotor speed, since the torque due to this force is much smaller than the aerodynamic braking torque. Hence equation (1) is taken as the speed function for the run down.
g) Coulomb friction is assumed for the friction force between rotor and inner race.

Considering these assumptions the nonlinear forces in radial and circumferential direction can be expressed as follows:

$$\begin{aligned} F_r &= 0 && r < s_1 \\ F_r &= -k_1 (r - s_1) - d_1 \dot{r} \cos\alpha && s_1 < r < s_2 \\ F_r &= -k_1 (s_2 - s_1) - k_2 (r - s_2) - d_2 \dot{r} \cos\alpha && r > s_2 \end{aligned} \tag{2}$$

$$\begin{aligned} F_\phi &= 0 && r < s_1 \\ F_\phi &= -d_\phi \dot{r} \sin\alpha - \mu F_r && \Omega_{ring} < \Omega_{rotor} \text{ and } r > s_1 \\ F_\phi &= -d_\phi \dot{r} \sin\alpha && \Omega_{ring} = \Omega_{rotor} \text{ and } r > s_1 \end{aligned} \tag{3}$$

r rotor displacement
$\dot{r}$ rotor velocity
α angle between rotor velocity and displacement
F_r bearing force on the rotor in radial direction (= direction of the rotor displacement)
F_ϕ bearing force on the rotor in circumferential direction
k_1 combined ball bearing and corrugated ribbon stiffness (two springs in series mode)

k_2 ball bearing stiffness alone (= auxiliary bearing stiffness if corrugated ribbon is flat)
d_1 combined ball bearing and corrugated ribbon damping in radial direction (two dampers in series mode)
d_2 ball bearing damping alone in radial direction (= auxiliary bearing damping if corrugated ribbon is flat)
d_ϕ corrugated ribbon damping in circumferential direction
s_1 radial gap between rotor and inner race
s_2 radial gap between rotor and inner race plus radial displacement of the outer race until the corrugated ribbon is flat
μ friction coefficient between rotor and inner race
Ω_{ring} angular velocity of the inner race
Ω_{rotor} angular velocity of the rotor

Ω_{ring} is calculated by integration of the following equation:

$$\Theta_{ring}\,\dot{\Omega}_{ring} = \mu\ R\,F_r \tag{4}$$

Θ_{ring} polar moment of inertia of the inner race including balls and cage
R inner radius of the inner race

Fig. 3 explains the damping effect of the corrugated ribbon in radial and circumferential direction. As the rotor moves in radial direction, the resulting force from the ribbon to the bearing (damping and stiffness), hence on the rotor have the direction of the rotor deflection (fig. 3a). This is not the case, if the rotor moves in circumferential direction (fig. 3b). An additional force F_2 (arbitrarily assumed in the figure) arises. This forces is only present, if the rotor moves in this direction, hence it is a damping force. The resulting force F_3 from the ribbon on the bearing, which is also the force from the bearing on the rotor, now also has a component in circumferential direction, which is vertical to the rotor deflection.

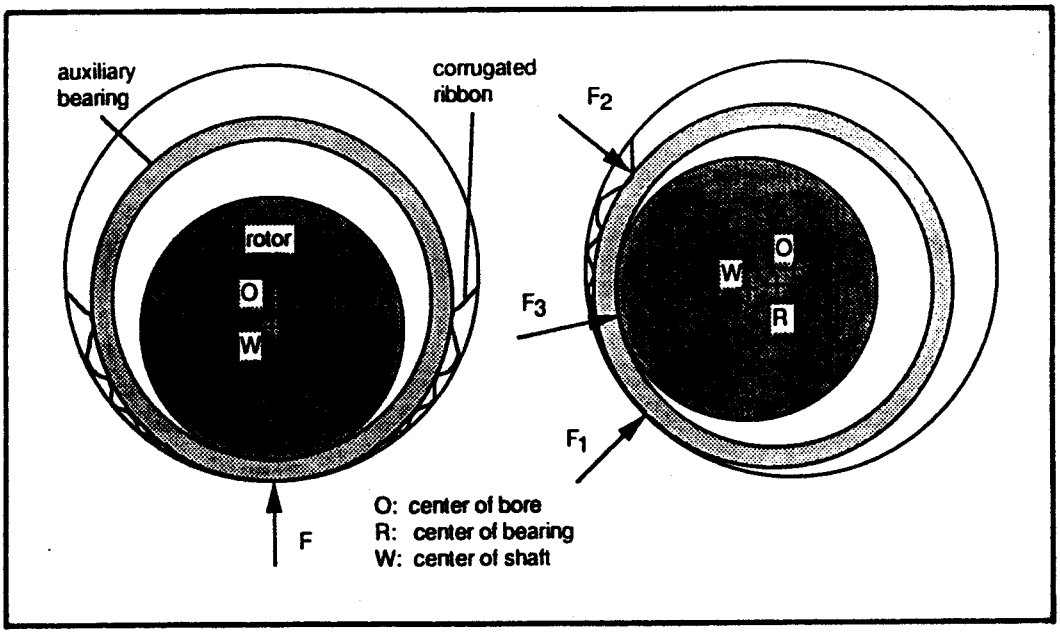

Figure 3. Forces from the corrugated ribbon on the bearing

The corresponding damping coefficient in circumferential direction may depend on the radial deflection, what is not taken into account. It may also be a function of the circumferential speed, as the radial damping coefficient may be a function of displacement and velocity. However, since all this is not exactly known, the model is simplified in the above described way.

Other investigators like T. Ishii and R.G. Kirk [2] assume an isotropic damping for the support of the outer ring in the housing. As the considerations above show this must not necessarily be the case for our design. They also take into account the lateral inertia of the auxiliary bearing, which does not seem to influence their results, and the torque on the rotor due to the friction, which in our case of a one ton rotor can be neglected (assumption f).

DETERMINING THE STIFFNESS AND DAMPING COEFFICIENTS

The stiffness coefficient of the corrugated ribbon was chosen according to data of S2M. This stiffness was assumed as k_1 (ribbon and bearing in series mode), since the ribbon is much softer.

In order to estimate the stiffness and damping coefficients of the ball bearing (k_2, d_2), the time history of the rotor being dropped into the auxiliary bearings at standstill was measured with the magnetic bearing sensors. It is shown in fig. 4. To identify the coefficients a simple one mass model according to fig. 5 is used in a first step. The corrugated ribbon is neglected in this model.

One way to determine the stiffness k_2 is from $\Delta x = A - s_2$, that is the amount by which the spring is pressed. This yields the following formula for k_2:

$$k_2 = s_2 \, g \, m_{rotor} / \Delta x^2 \qquad (5)$$

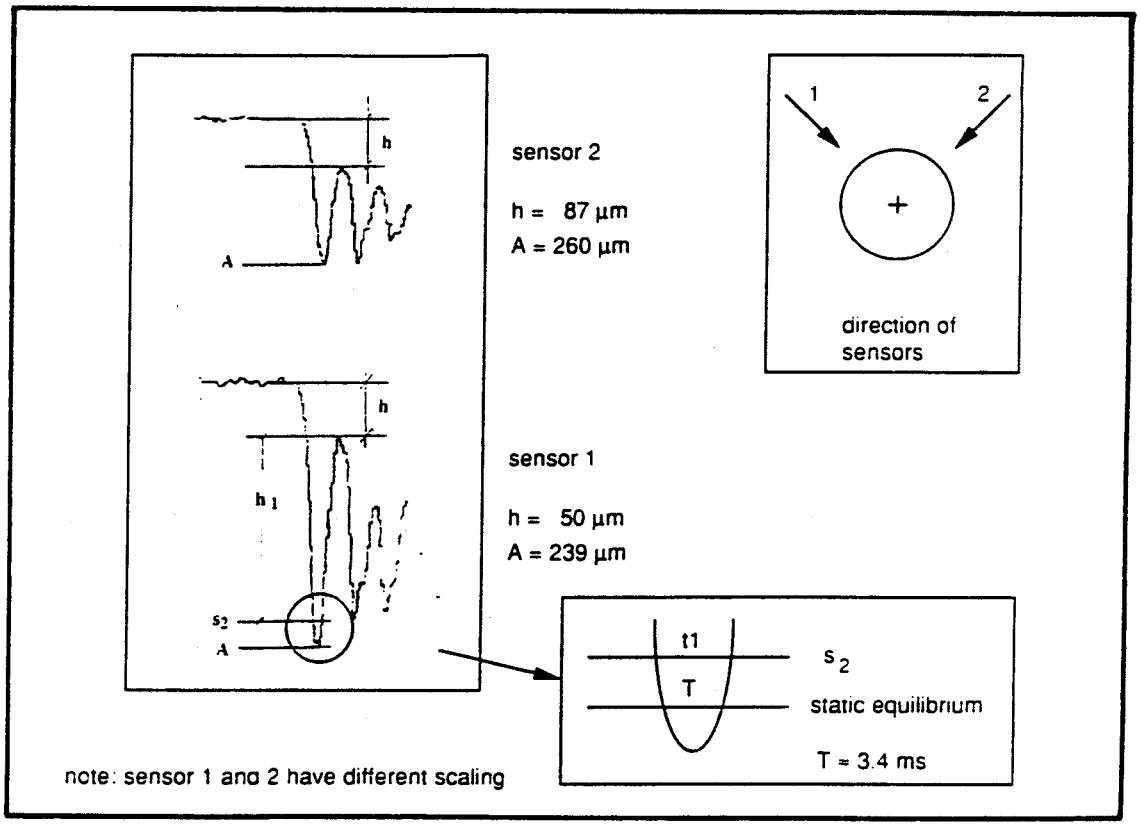

Figure 4. Measured time history of a drop at standstill

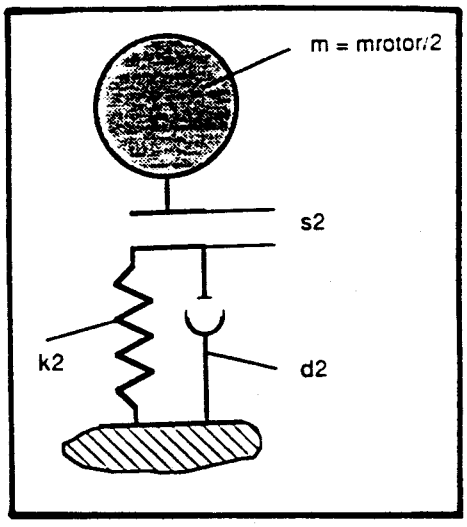

Figure 5.
Simple one mass model for the stiffness and damping identification

Another way to determine this stiffness from the simple one mass system is by the impact duration T (see fig.4), which is half the period of the natural frequency of the one mass system ($\omega_k=\sqrt{2k_2/m_{rotor}}$). Since the static deflection (hence the reading of T) also depends on the stiffness, the estimation has to be done in a iterative manner. Both methods yield about the same value.

The damping coefficient d_2 is identified from the maximum rebound.

The identified stiffness and damping coefficients for the ball bearings (see table I) are in the same order of magnitude as those in [3].

The damping coefficient of the corrugated ribbon can be determined from damping factors according to the following formula, which is a quite common way to include hysteretic damping in mechanical systems:

$$d_{CR} = 2D_{CR}\, k_1 / \omega \qquad (6)$$

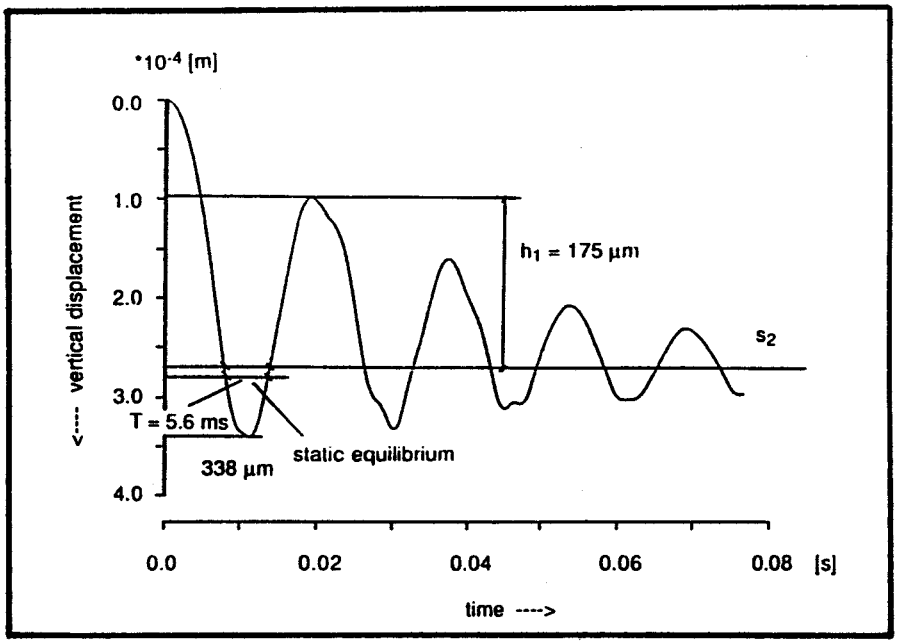

Figure 6. Calculated time history of the rotor drop at standstill

A damping factor D_{CR} of 15% and a frequency of ω=350rad/s (= natural frequency of half the rotor mass supported on the corrugated ribbon, which is an assumed value for the frequency of the dominating vibration) yield a value for d_{CR}, which is slightly above d_2. Hence a radial damping coefficient d_1 (combined ball bearing and ribbon damping, two dampers in series mode) equal to d_2 will not be far from reality. In the further investigations we assume this value for d_1.

In the next step a calculation of the rotor being dropped at stand still was carried out with the complete finite element model and the above determined stiffness and damping coefficients, which are listed in table I. Fig. 6 shows the result. The coincidence with the measured time history was considered as sufficient, so we did not try to improve it by further changing the coefficients.

For the circumferential damping coefficient d_ϕ, which has practically no influence on the vibrational behaviour of a drop at standstill, a value of the same order of magnitude as for the radial damping coefficient seems to be realistic. However, since it is not exactly known, this value is varied in the following investigations.

The natural frequency of the ball bearing alone supported on the corrugated ribbon is about 1000 Hz. This shows that our assumption of neglecting the lateral inertia of the bearing is valid, since the dominating effects of the rotor drop are in a much lower frequency range.

Our damping coefficients are far below the optimal value (only about 5%-10% of this value), which can be determined according to a formula given in [2]. However damping coefficients in the order of magnitude of our values, above all for the circumferential direction, are sufficient, as our results will show, and can be achieved with a simple corrugated ribbon.

THEORETICAL RESULTS

All results presented here and also in the previous paragraph were calculated with the nonlinear part NOLIN of the rotor dynamic programme package MADYN [4].

All values for the parameter of the auxiliary bearing are shown in table I. The unbalance of the rotor was assumed according to the unbalance during the tests (see next paragraph), that is an unbalance of 0.005kgm in the rotor middle and 0.0018kgm at each impeller. All unbalances are in the same direction. The unbalance and also the initial conditions (that is the position and velocity of the shaft, which is vibrating in a steady state condition, at the instant of the magnetic bearing failure) do not have a big influence on the results, as long as the unbalance has a normal order of magnitude.

TABLE 1 - Bearing parameter

Parameter	value	determined by	variation range
s_1 [mm]	170	given design	-
s_2 [mm]	250	given design	150 - 350
R [mm]	95	given design	-
Θ_{ring} [kgm^2]	0.02	given design	0.01 - 0.02
μ	0.5	assumption	0.3 - 0.8
k_1 [N/m]	5.7 10^7	measurement	-
k_2 [N/m]	4.3 10^8	measurement	10^8 - 10^9
d_1 [Ns/m]	4.3 10^4	ass., meas.	-
d_2 [Ns/m]	4.3 10^4	measurement	-
d_ϕ [Ns/m]	0	assumption	0 - 4.3 10^4

Fig.7 shows the orbit of the rotor in the auxiliary bearings at the thrust end side for a drop at almost full speed without circumferential damping. The figure shows, how the rotor is accelerated in revers direction due to the friction and how it starts whirling. Because of the whirling the auxiliary bearing is loaded with centrifugal forces, which are about six times the bearing load due to the weight. The magnitude of the centrifugal force is determined by the frequency (app. 63 Hz) and radius of the whirling. This high load can destroy the bearing, if it acts for an extended period of time.

This result shows how important the circumferential damping of the corrugated ribbon is. If there is no circumferential damping as in our example, the whirling goes on indefinitely. A damping coefficient of $d_\phi = 1\ 10^4$ Ns/m, which is a much smaller value than the coefficient in radial direction, stops the whirling after 7 cycles (see fig. 8). In case of higher values the rotor does not start whirling at all.

In case of very large unbalances (five times higher than in our investigation) the rotor may also start whirling in forward direction.

Fig. 9 to 12 show the influence of the clearance s_2, the ball bearing stiffness k_2, the moment of inertia of the inner ring Θ and the friction coefficient μ on the radius and frequency of the whirling. It can be seen that decreasing the clearance or increasing the stiffness reduces the whirling radius and increases the frequency. These two effects have an opposite influence on the centrifugal force. The resulting centrifugal force is lower in the case of smaller clearance and higher in the case of larger stiffness. Decreasing the friction and the inner ring inertia decreases both, the radius and the frequency. For values below those in the figures a whirling is even prevented.

In all presented results the rotor whirls in a parallel mode with a frequency below the first natural frequency of the rotor supported on the auxiliary bearings (corrugated ribbon flat). The rotor can not whirl above this frequency in a parallel mode, since in such a case it would have the tendency to center itsself and would no longer be in contact with the inner race. In case it whirls in a conical mode the whirling frequency could be higher. However it is not yet clear, under which conditions such a whirling occurs.

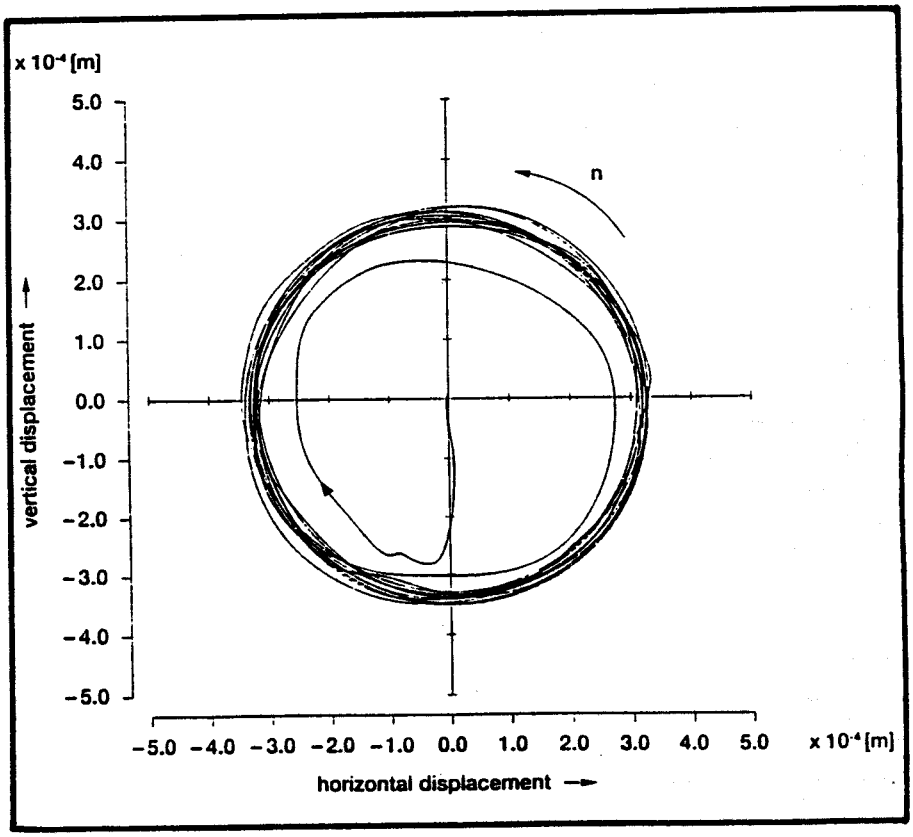

Figure 7.
Calculated orbit of the rotor being dropped at full speed, no circumferential damping

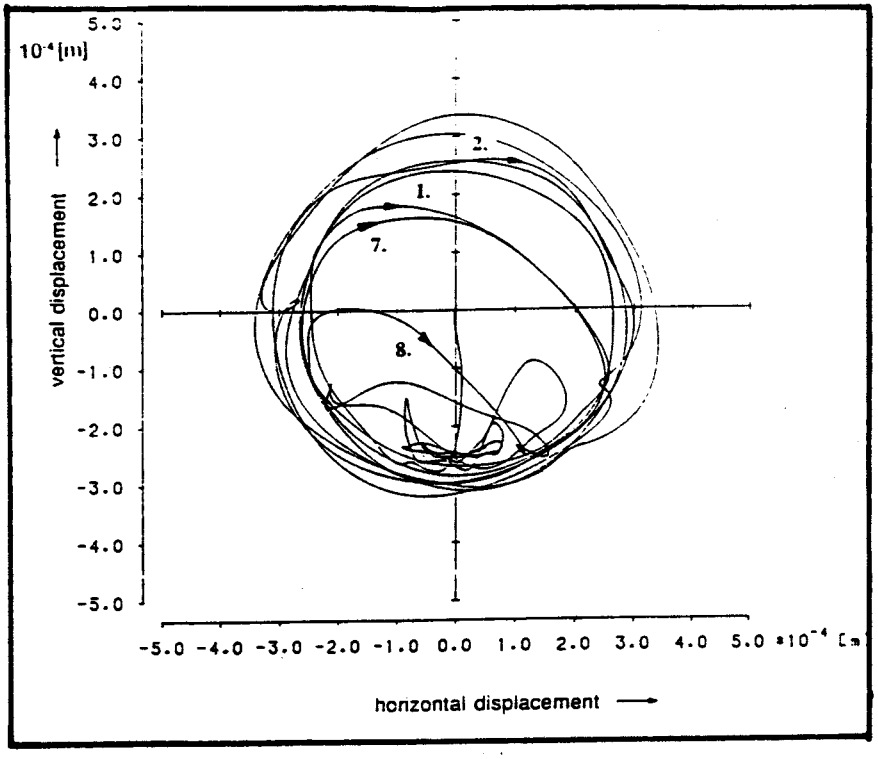

Figure 8.
Calculated orbit of the rotor being dropped at full speed, circumferential damping $d_\phi=10^4$ Ns/m

TEST RESULTS

The drop test was carried out at almost full speed (n=9300rpm) and almost full load. The rotor was dropped by switching off the magnetic bearing amplifiers. The motor was shut down simultaneously.

Fig.13 shows the measured orbit at the thrust end auxiliary bearing. The rotor also starts whirling but stops after seven cycles. The whirling frequency is app. 37Hz. The maximum deflection is much larger than in the calculation. This is because the auxiliary bearing was mounted slightly eccentric, when the test was carried out. However what is completely surprising is the whirling direction. It is not in the reverse direction to the rotation of the shaft as was expected from the simulation. The rotor whirls in the same direction as the shaft rotates.

This can not be explained by a large unbalance, since the unbalance was approximately as assumed in the simulation. For a much larger unbalance it would not have been possible to operate the rotor in magnetic bearings at 9300rpm.

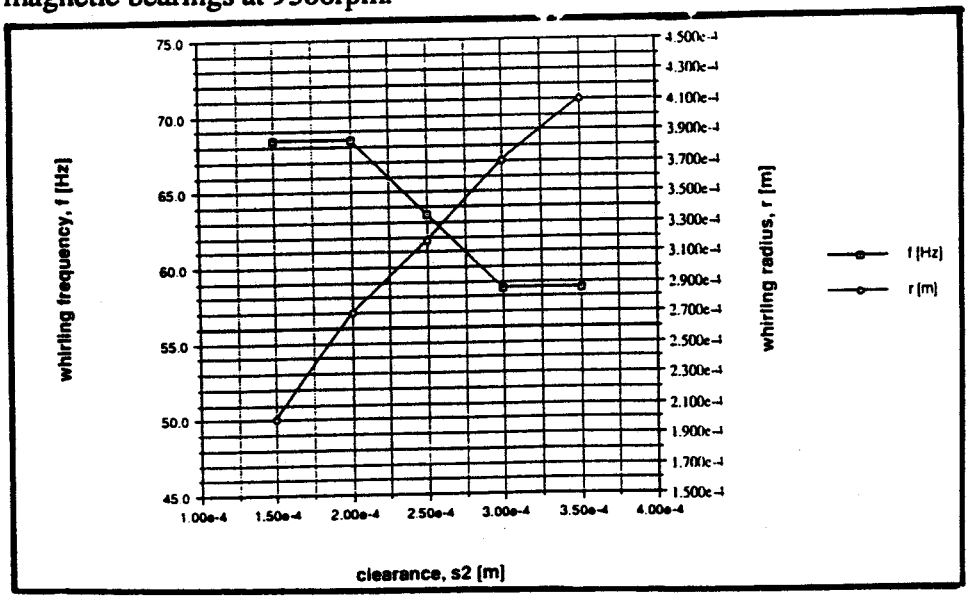

Figure 9.
Influence of different clearances s_2 on the whirling radius and frequency

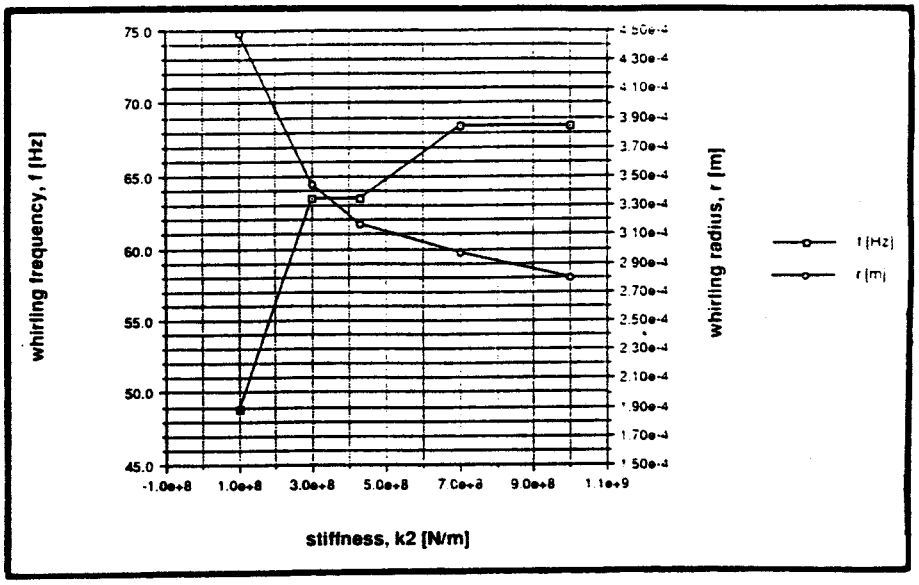

Figure 10.
Influence of different stiffness k_2 on the whirling radius and frequency

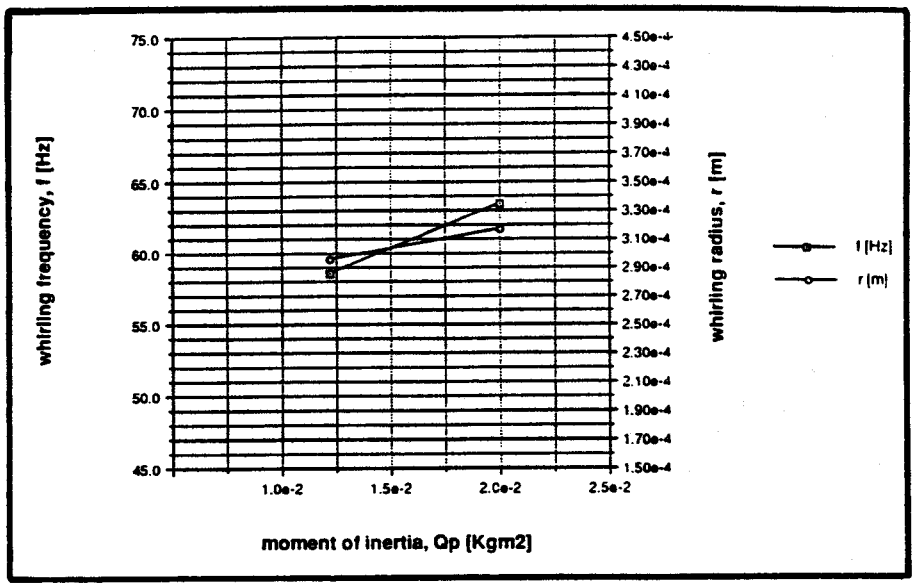

Figure 11.
Influence of different moments of inertia of the inner ring on the whirling radius and frequency

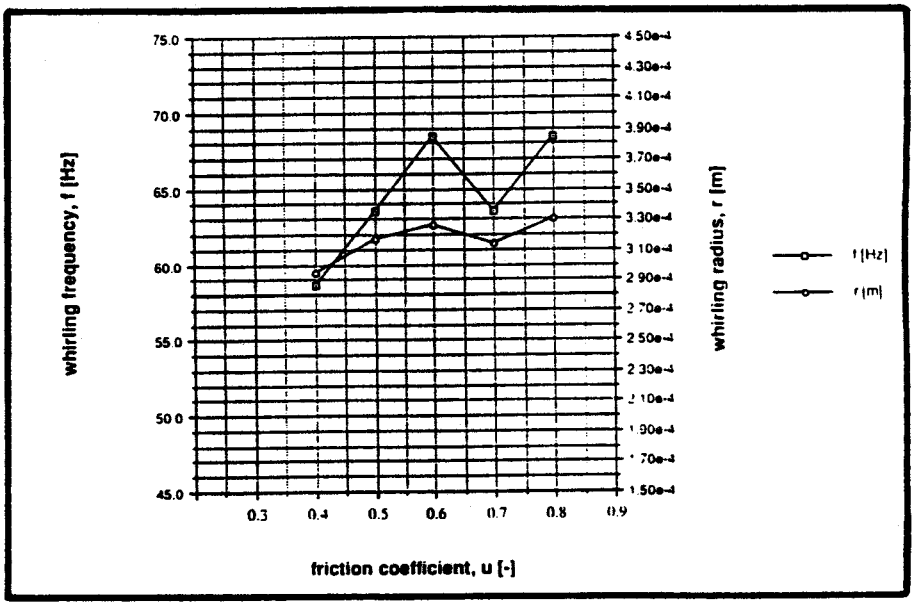

Figure 12.
Influence of different friction coefficients m on the whirling radius and frequency

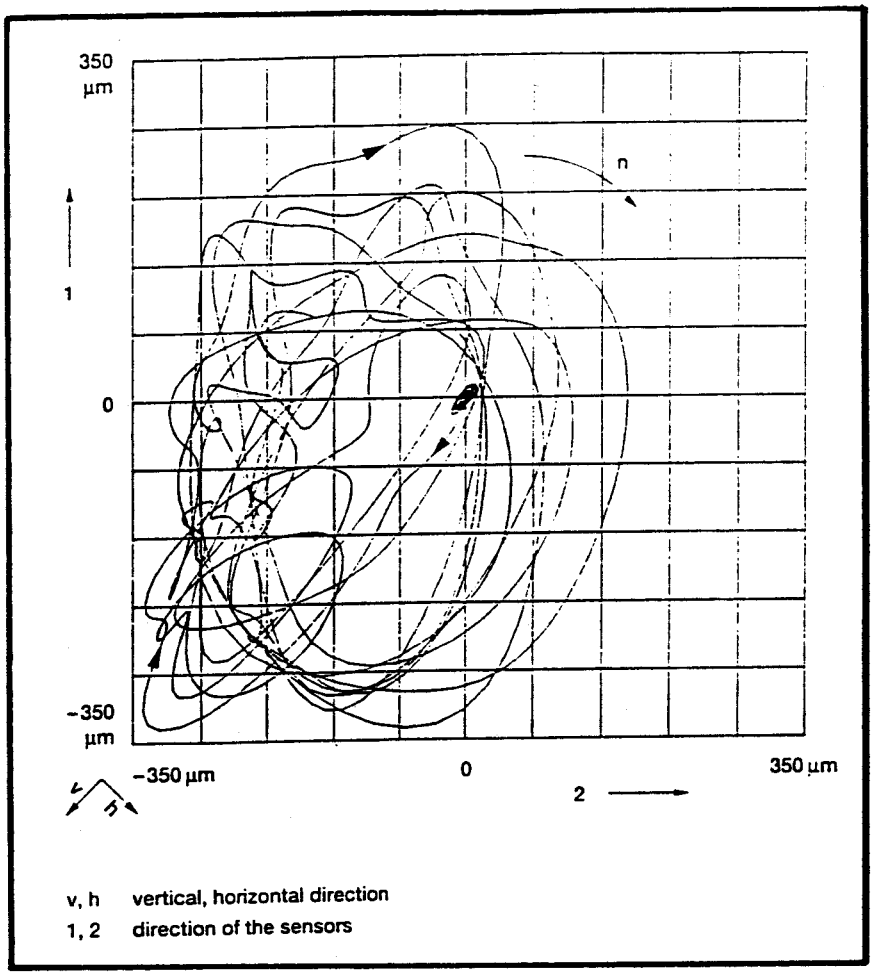

Figure 13.
Measured orbit of the rotor being dropped, n=9300 rpm

Other possible forces to compel the rotor to whirl in forward direction are labyrinth seal forces and electromagnetic forces in the motor. The labyrinths however are too small, as a calculation including the labyrinths modeled according to [5] showed.

Electromagnetic forces will still be present due to the collapsing electromagnetic fields after the motor shut down. One has to consider also, that the time from switch off to the end of the whirling is only a few tenths of a second and that the manual motor shut down could have been slightly later.

From [6] is known, that lateral vibrations in induction motors with a squirrel cage may cause cross coupling forces. To force the rotor in forward direction a cross coupling stiffness in the order of magnitude of 10^7 N/m in the middle of the rotor is necessary. An estimation of the cross coupling stiffness according to [6] at nominal conditions of the motor for a dropping rotor (the value also depends on the kind of deflection of the rotor) yields a value of about one third of the required cross coupling stiffness. A cross coupling stiffness due to the collapsing field can not be estimated. The formulas in /6/ however show that much larger values are possible. Further tests to clarify the cause of the forward whirling will be carried out. They were not possible up till now, since the machine had to be removed from the test stand right after the test before the results could be evaluated.

CONCLUSIONS

The most severe condition that can occur, if the rotor drops into the auxiliary bearings at full speed and full load, is a whirling with approximately the clearance between ball bearing and rotor as the radius. It is caused by an acceleration of the rotor in revers direction due to the friction between inner ring and rotor and generates a very high load on the auxiliary bearing.

Very large unbalances in an order of magnitude, which can not occur in normal operation, or other forces like aerodynamic forces, or electromagnetic forces from a motor can also compel the rotor to whirl in forward direction.

The whirling must be prevented or stopped after a short time. In our case this is achieved by a corrugated ribbon, which creates a circumferential damping. Other means to prevent a whirling is a sufficient low moment of inertia of the inner ring and a low friction coefficient between inner ring and rotor. Small clearances and a low ball bearing stiffness can reduce the load in case of a whirling.

REFERENCES

1. Schmied, J., 1990." Experience with Magnetic Bearings supporting a Pipeline Compressor." Proceedings of the second International Symposium on Magnetic Bearings in Tokyo.
2. Ishii, T., Kirk R.G., 1991." Analysis of Rotor Drop on Auxiliary Bearings Following AMB Failure." ROMAG 91, Conference on Magnetic Bearings and Dry Gas Seals.
3. Ophey, l., 1986." Dämpfungs und Steifigkeitseigenschaften vorgespannter Schrägkugellager." VDI-Z Bd.128 (1986) Nr. 12.
4. Klement, H.D., Pradetto, J.C., Schmied, J., 1989." Berechnung transienter Schwingungen von Modellen mit örtlichen Nichtlinearitäten am Beispiel des Notauslaufs eines Rotors mit Magnetlagern." VDI Berichte 786.
5. Wyssmann, H.R., Pham, T.C. and R.J. Jenny, 1984."Prediction of Stiffness and Damping Coefficients for Centrifugal Compressor Labyrinth Seals." ASME Journal of Engineering for Gas Turbines and Power, Vol. 106.
6. Früchtenicht, J.,Jordan, H. and H.O. Seinsch, 1982."Exzentrizitätsfelder als Ursache von Laufinstabilität bei Asynchronmaschinen." Archiv für Elektrotechnik 65.